US 20220136937A1

(19) **United States**

(12) **Patent Application Publication** (10) **Pub. No.: US 2022/0136937 A1**

Deng et al. (43) **Pub. Date: May 5, 2022**

(54) **SILVER NANOPARTICLE SURFACE ENABLED SELF-ASSEMBLY OF ORGANIC DYE MOLECULES**

(71) Applicant: **Morgan State University**, Baltimore, MD (US)

(72) Inventors: **Hua Deng**, Baltimore, MD (US); **Hongtao Yu**, Baltimore, MD (US)

(21) Appl. No.: **17/401,985**

(22) Filed: **Aug. 13, 2021**

Related U.S. Application Data

(60) Provisional application No. 63/065,112, filed on Aug. 13, 2020.

Publication Classification

(51) **Int. Cl.**

G01N 1/30	(2006.01)
C09B 62/44	(2006.01)
C09K 11/06	(2006.01)

(52) **U.S. Cl.**

CPC ***G01N 1/30*** (2013.01); ***C09B 62/44*** (2013.01); *G01N 2001/302* (2013.01); *C09K 2211/1018* (2013.01); *C09K 2211/1007* (2013.01); ***C09K 11/06*** (2013.01)

(57) **ABSTRACT**

Fluorescence titration of methylene blue, rhodamine B and rhodamine 6G (R6G) by silver nanoparticle (AgNP) all resulted in an initial steep quenching curve followed with a sharp turn and a much flatter quenching curve. At the turn, there are about 200,000 dye molecules per a single AgNP, signifying self-assembly of approximately 36 layers of dye molecules on the surface of the AgNP to form a micelle-like structure. These fluorescence-quenching curves fit to a mathematical model with an exponential term due to molecular self-assembly on a AgNP surface, or "self-assembly shielding effect", and a Stern-Volmer term (nanoparticle surface enhanced quenching). Such a "super-quenching" by AgNP can only be attributed to "pre-concentration" of the dye molecules on the nanoparticle surface that yields the formation of micelle-like self-assembly, resulting in great fluorescence quenching. Overall, the fluorescence quenching titration reveals three different types of interactions of dye molecules on AgNP surface: 1) self-assembly (methylene blue, rhodamine B and R6G), 2) absorption/tight interaction (tryptamine and fluorescein), and 3) loose interaction (eosin Y). We attribute the formation of micelle-like self-assembly of these three dye molecules on AgNP to their positive charge, possession of nitrogen atoms, and with relatively large and flat aromatic moieties.

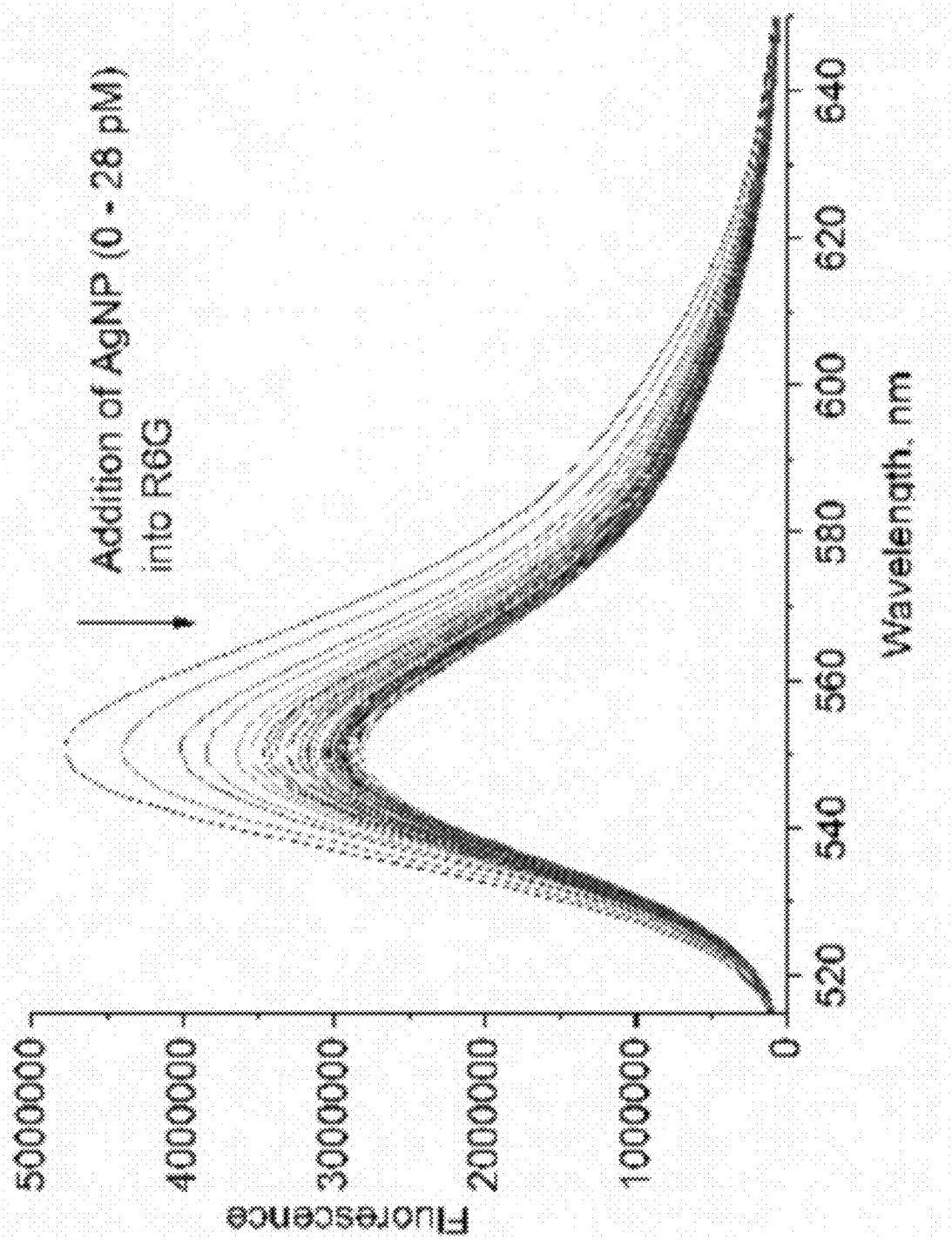
Addition of AgNP (0 - 28 pM)
into R6G
Fluorescence
5000000
4000000
3000000
2000000
1000000
0
520
540
560
580
600
620
640
Wavelength, nm

Figure 1A

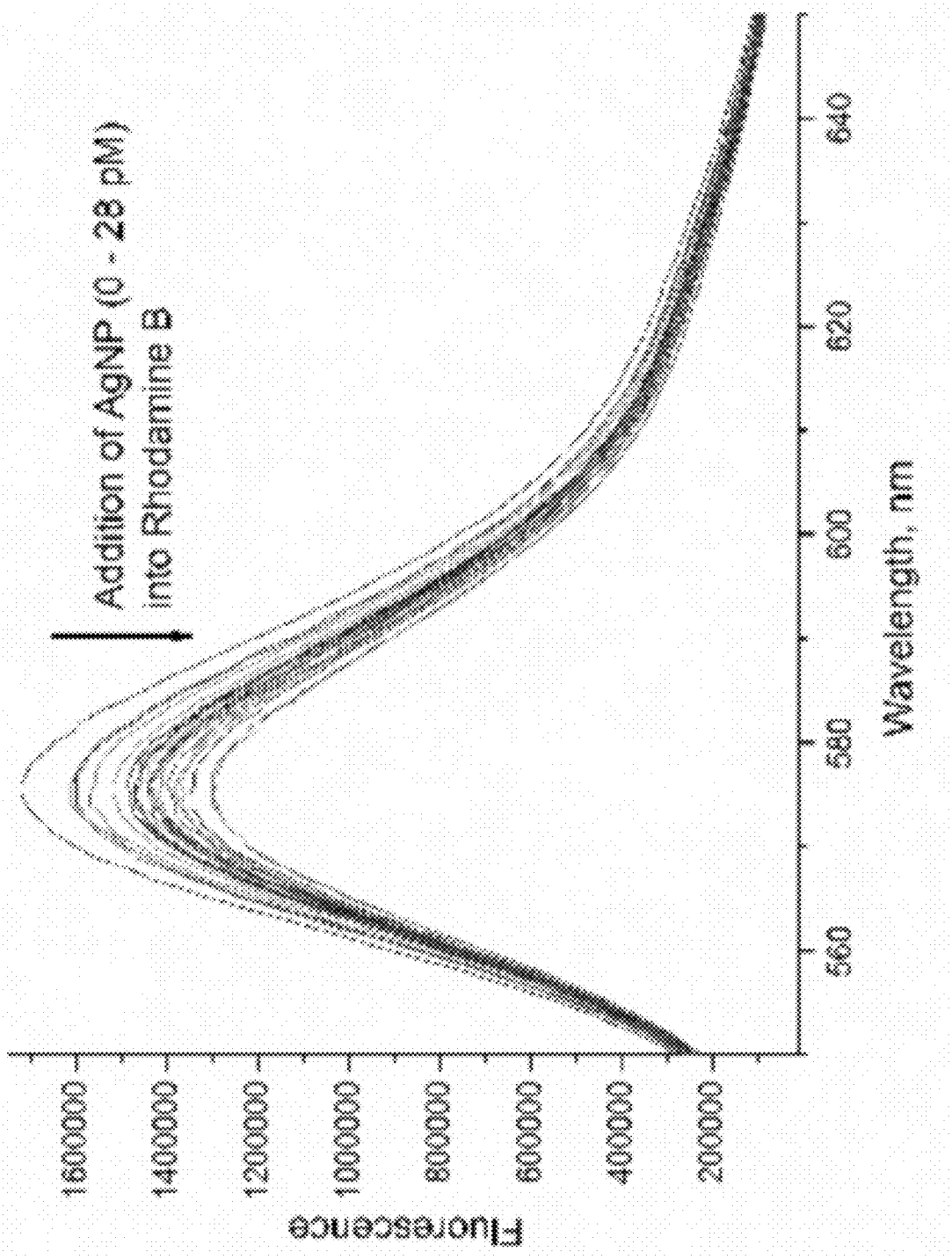
Addition of AgNP (0 - 28 pM)
into Rhodamine B
Fluorescence
1600000
1400000
1200000
1000000
800000
600000
400000
200000
560
580
600
620
640
Wavelength, nm

Figure 1B

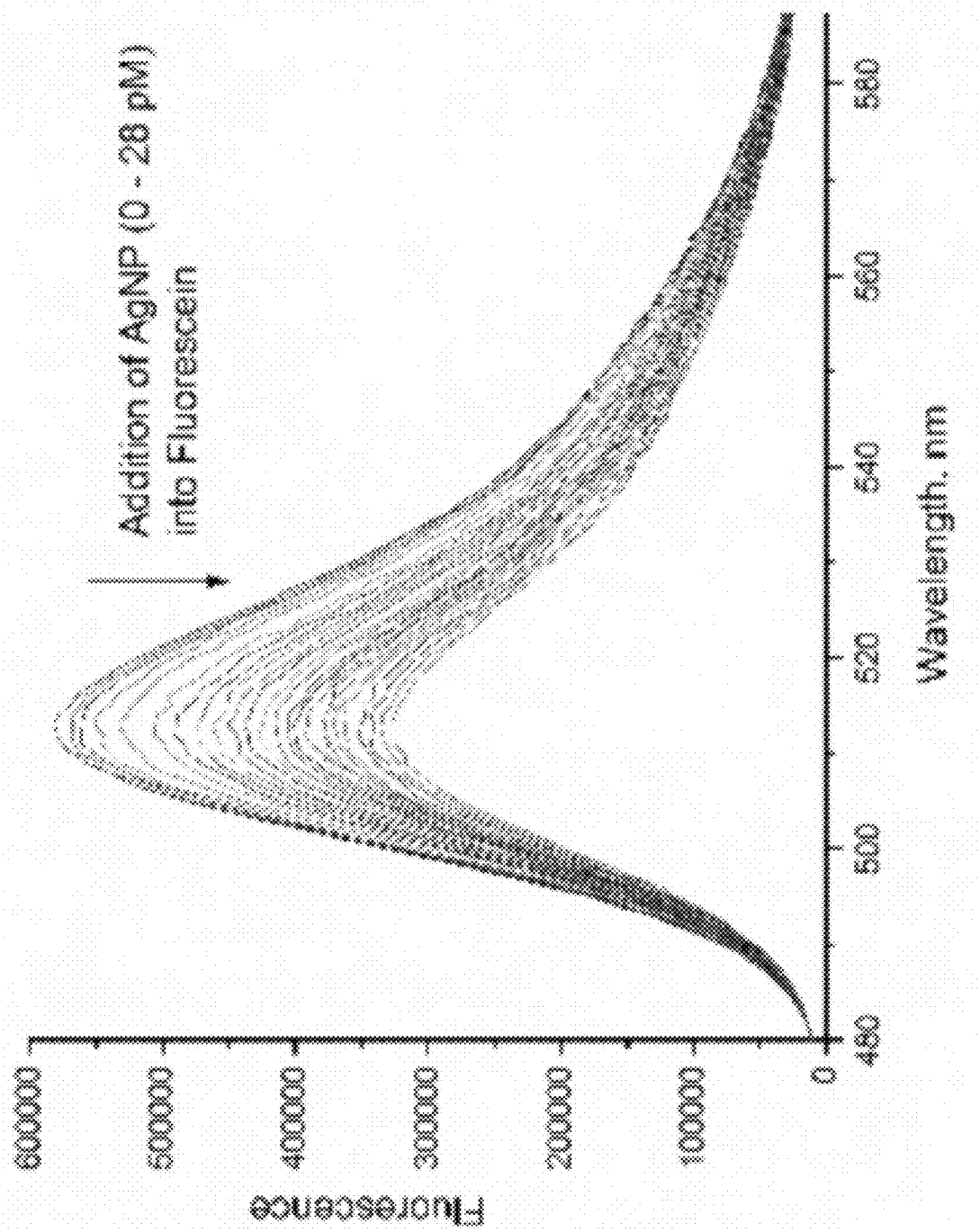
Addition of AgNP (0 - 28 pM)
into Fluorescein
Fluorescence
600000
500000
400000
300000
200000
100000
0
480
500
520
540
560
580
Wavelength, nm

Figure 1C

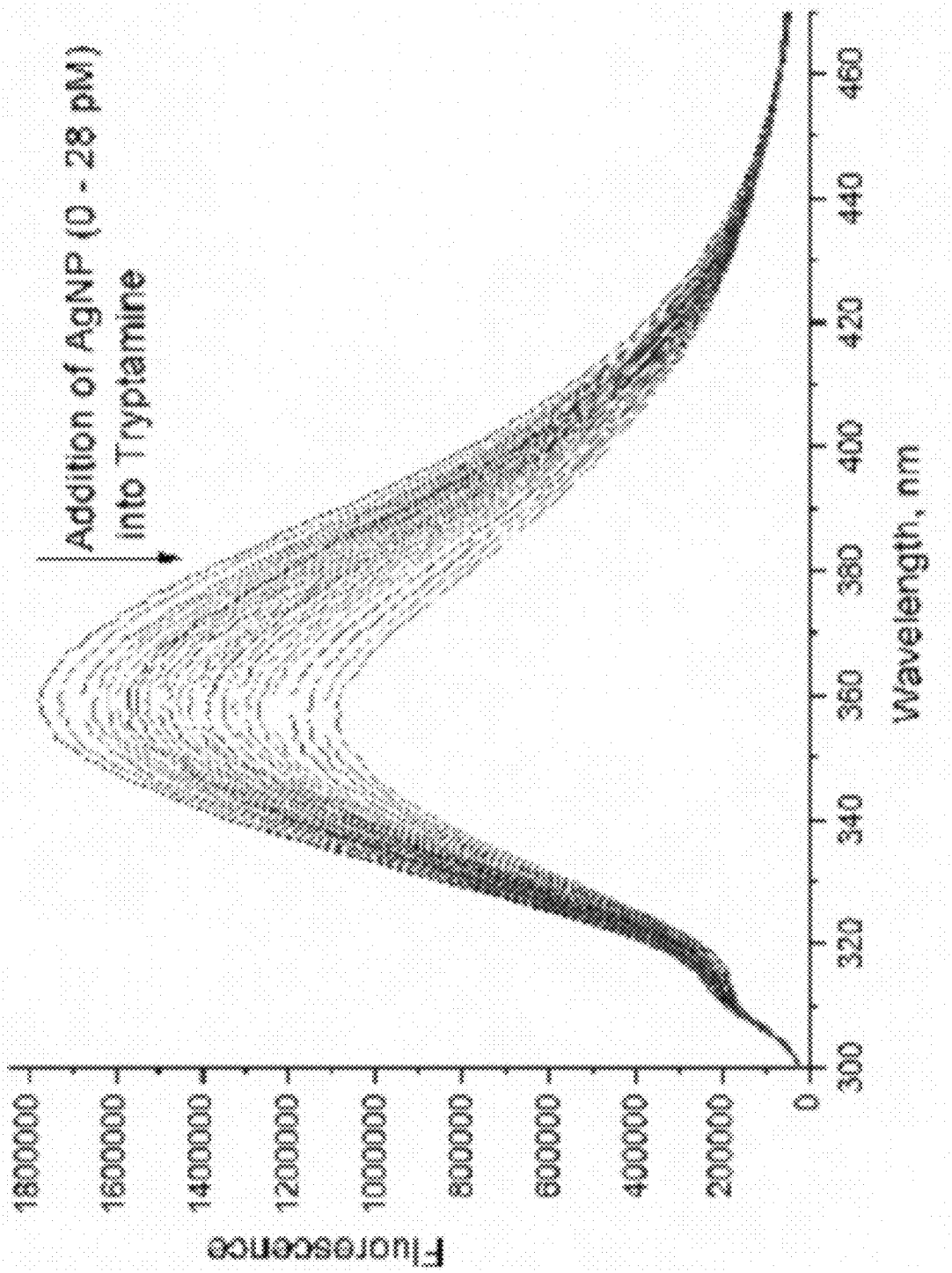
Addition of AgNP (0 - 28 pM)
into Tryptamine
Fluorescence
Wavelength, nm
1800000
1600000
1400000
1200000
1000000
800000
600000
400000
200000
0
300
320
340
360
380
400
420
440
460

Figure 1D

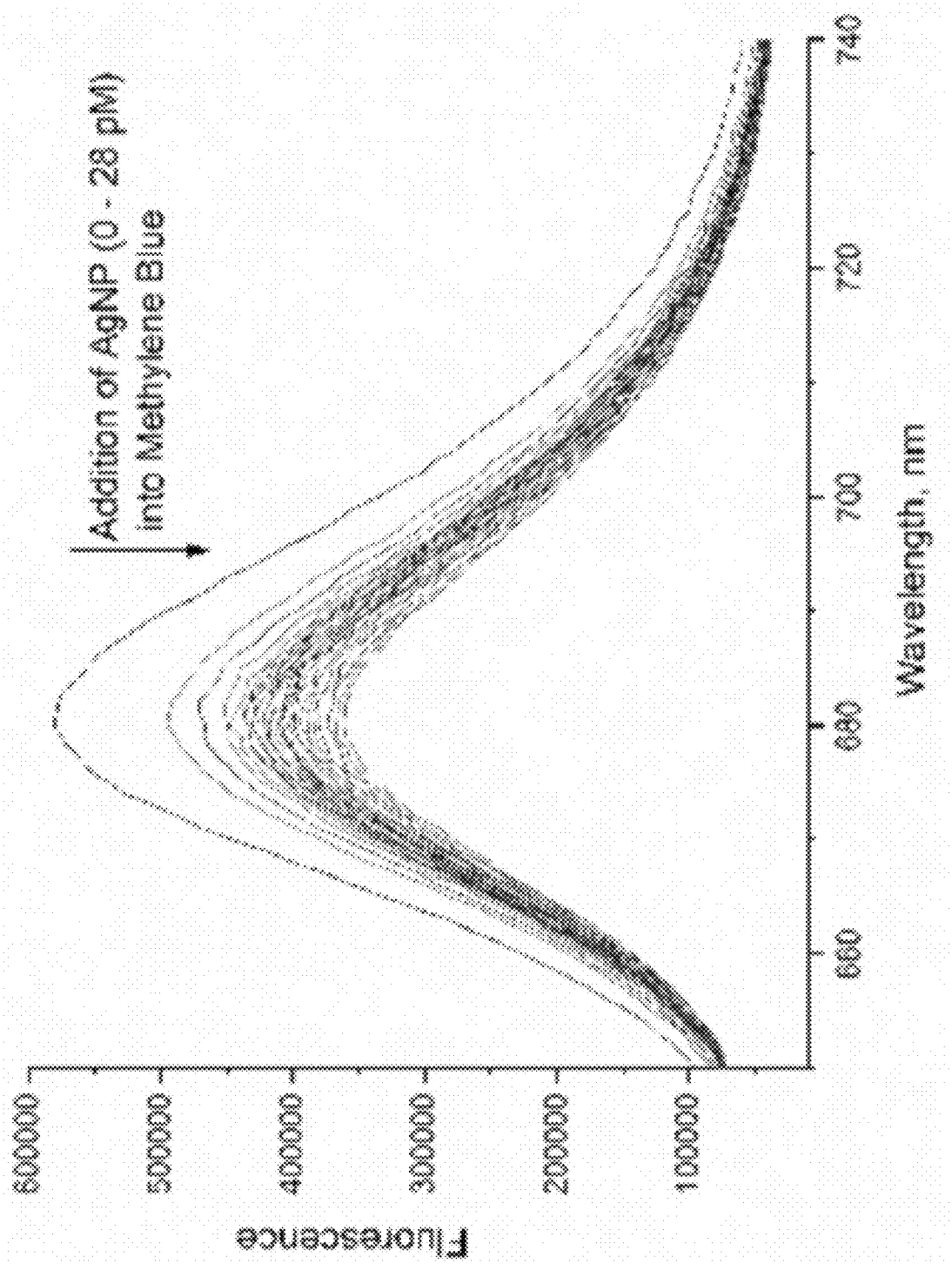
Addition of AgNP (0 - 28 pM)
into Methylene Blue
Fluorescence
600000
500000
400000
300000
200000
100000
600
640
700
720
740
Wavelength, nm

Figure 1E

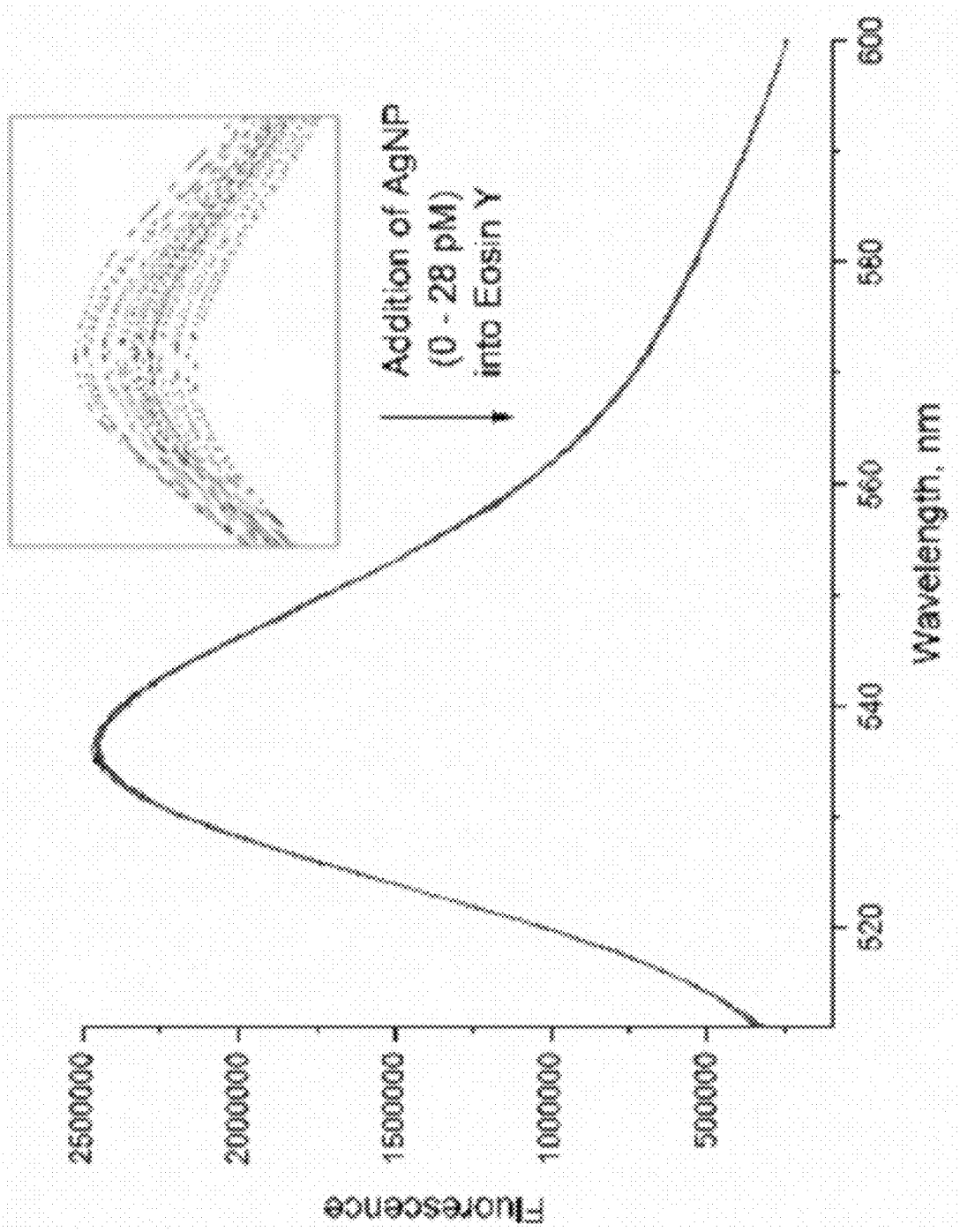
Addition of AgNP
(0 - 28 pM)
into Eosin Y
Fluorescence
2500000
2000000
1500000
1000000
500000
520
540
560
580
600
Wavelength, nm

Figure 1F

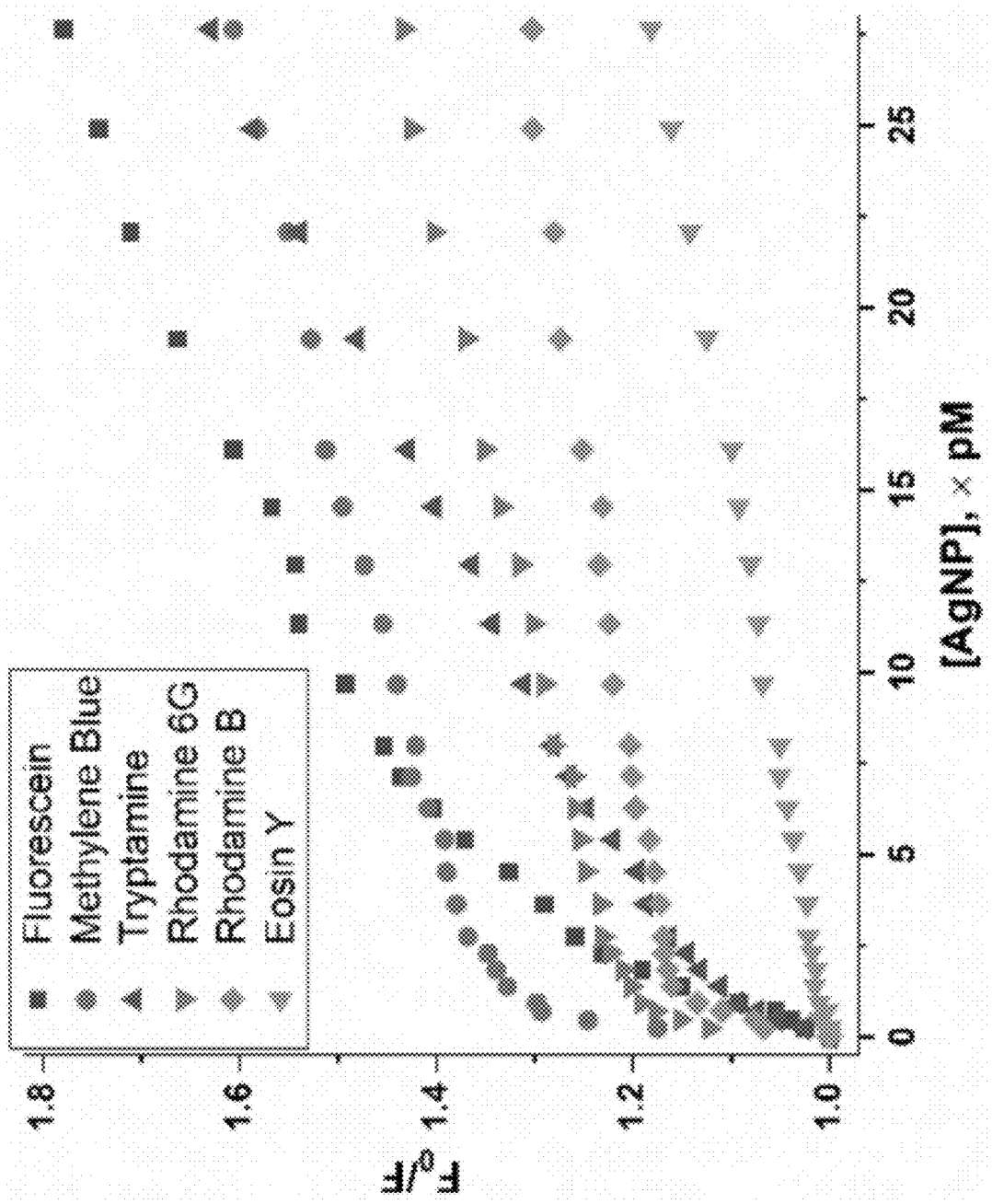
Fluorescein
Methylene Blue
Tryptamine
Rhodamine 6G
Rhodamine B
Eosin Y
F_0/F
1.8
1.6
1.4
1.2
1.0
0
5
10
15
20
25
[AgNP], × pM

Figure 2A

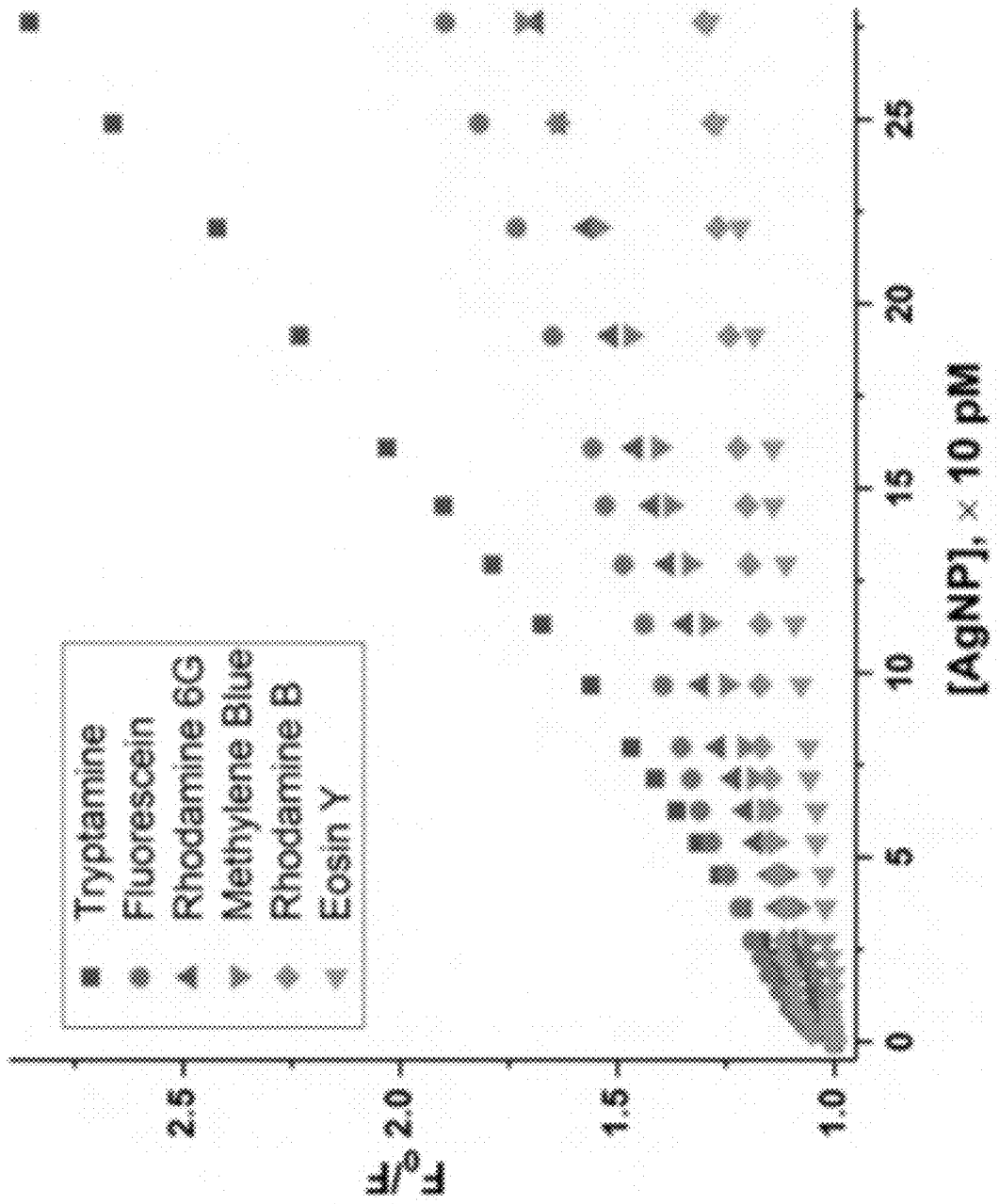
Tryptamine
Fluorescein
Rhodamine 6G
Methylene Blue
Rhodamine B
Eosin Y
F_0/F
2.5
2.0
1.5
1.0
0
5
10
15
20
25
[AgNP], × 10 pM

Figure 2B

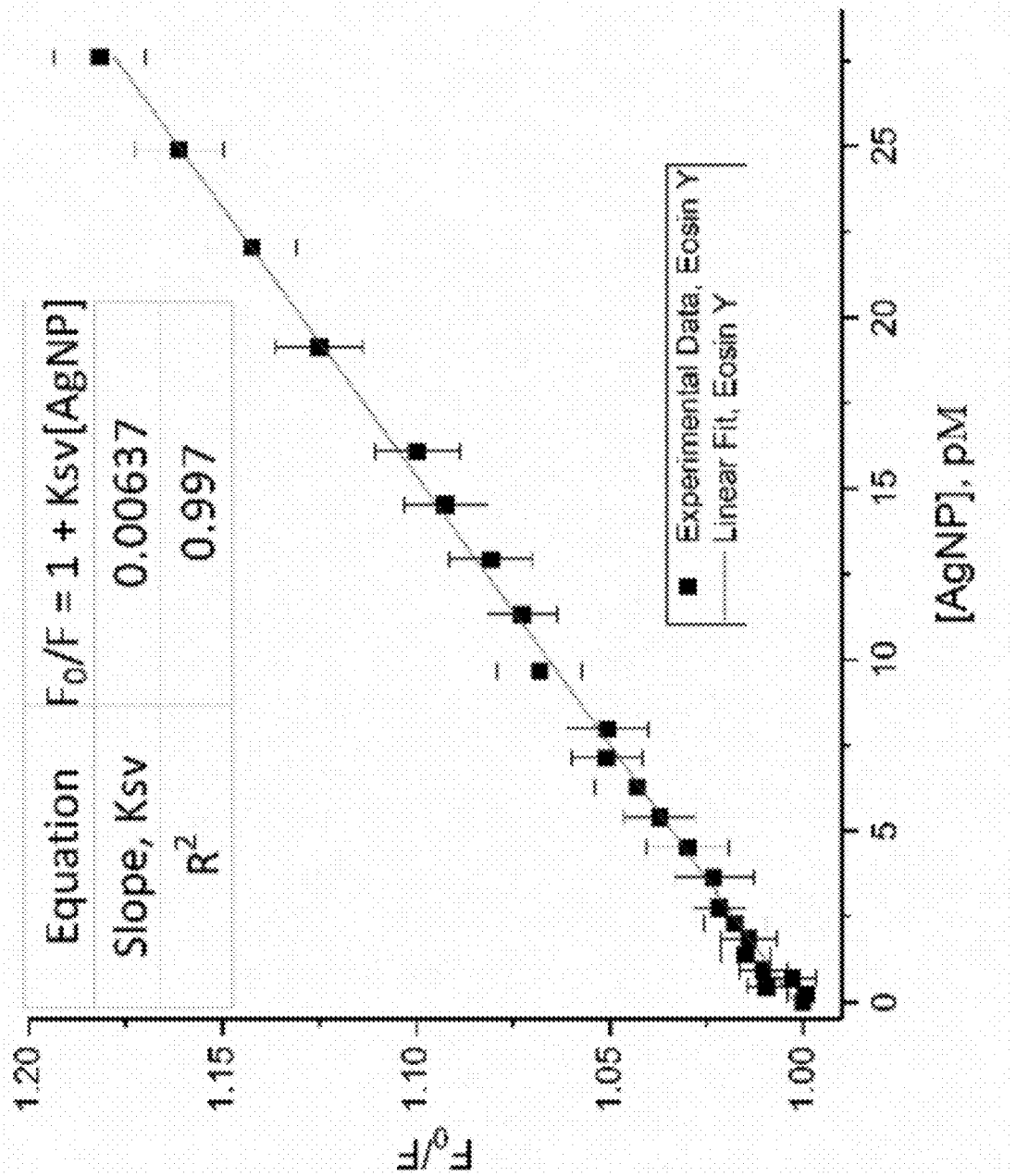
Equation $F_0/F = 1 + Ksv[AgNP]$
Slope, Ksv 0.00637
R^2 0.997
Experimental Data, Eosin Y
Linear Fit, Eosin Y
F_0/F
[AgNP], pM
1.20
1.15
1.10
1.05
1.00
0
5
10
15
20
25

Figure 3

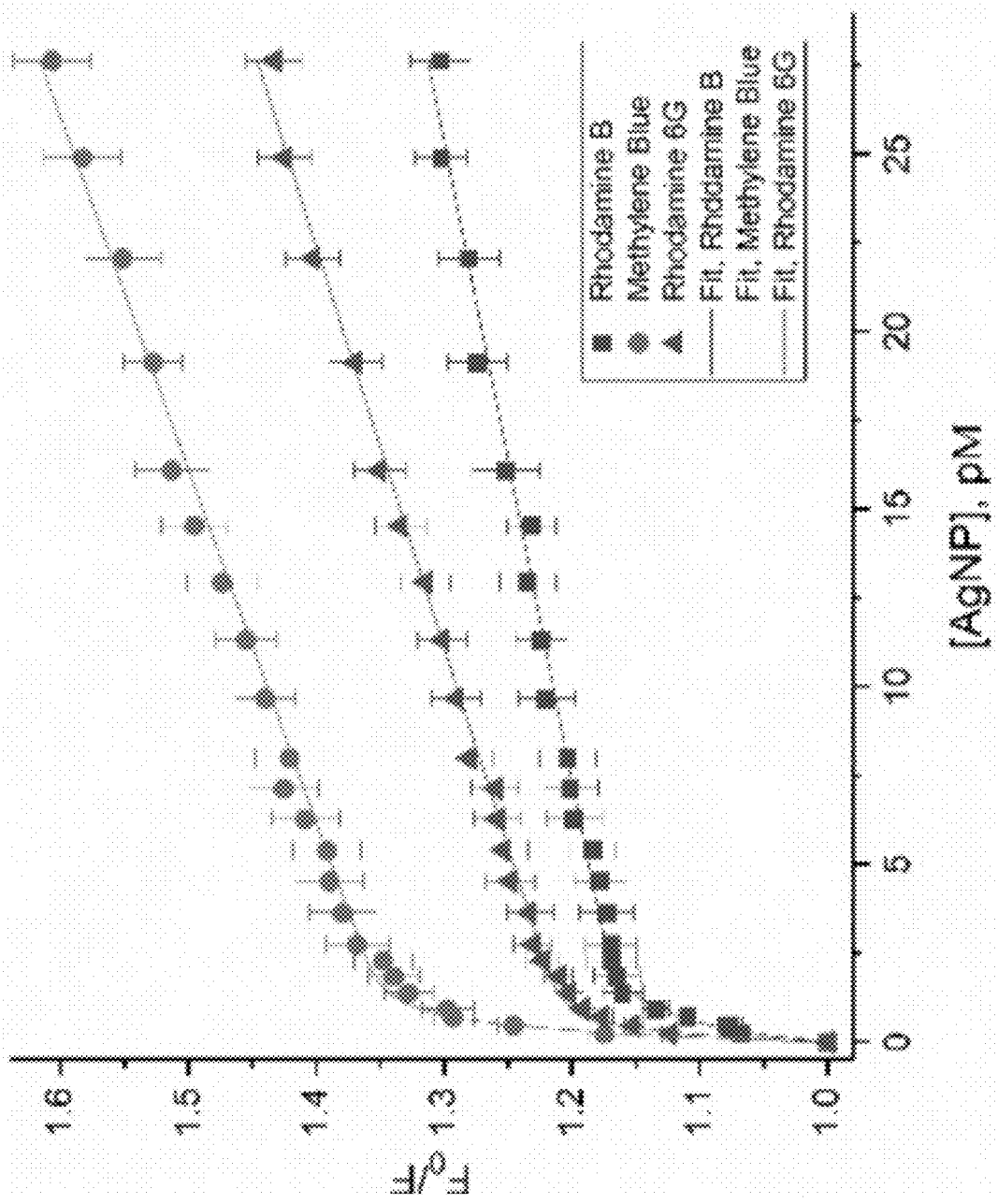
Rhodamine B
Methylene Blue
Rhodamine 6G
Fit, Rhodamine B
Fit, Methylene Blue
Fit, Rhodamine 6G
F_0/F
[AgNP], pM
1.0
1.1
1.2
1.3
1.4
1.5
1.6
0
5
10
15
20
25

Figure 4A

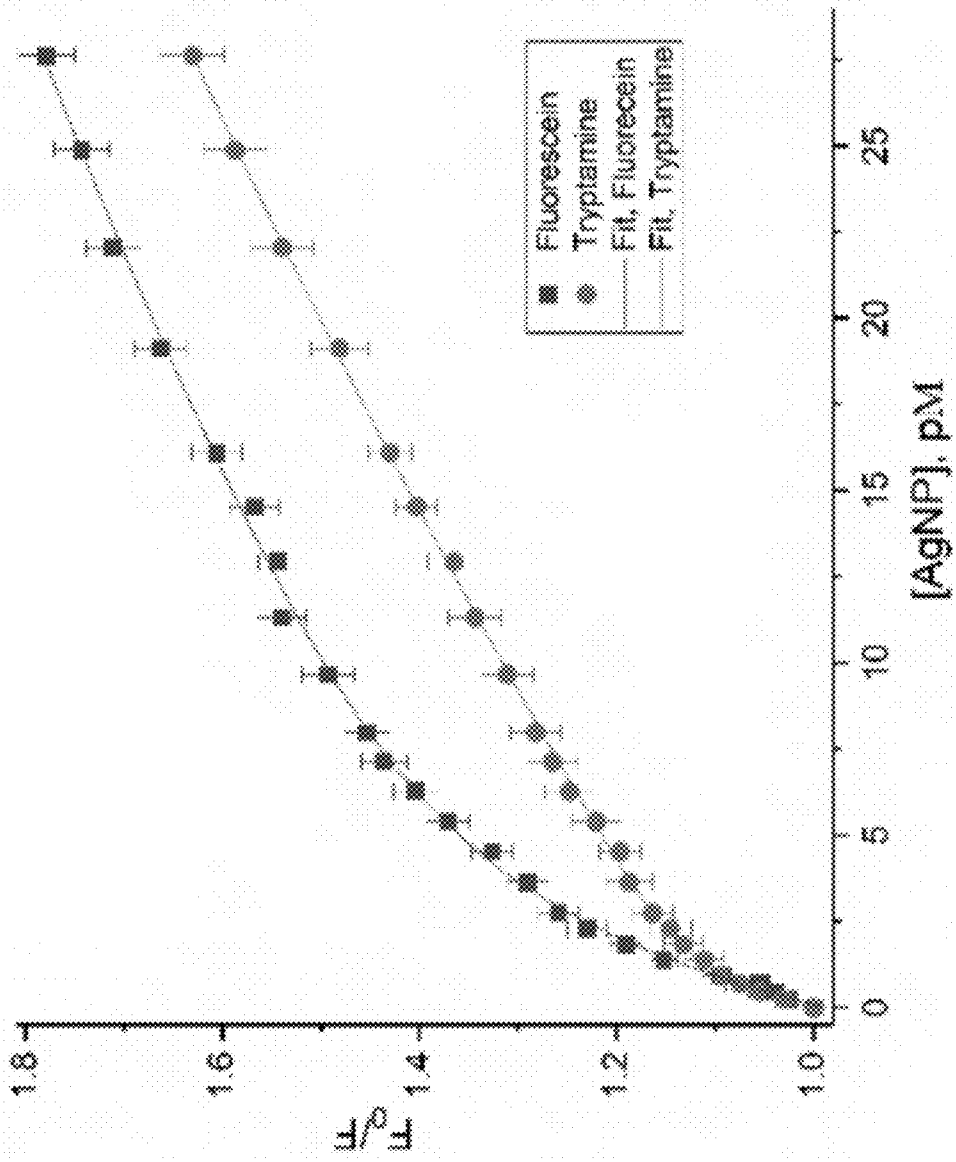
Fluorescein
Tryptamine
Fit, Fluorescein
Fit, Tryptamine
F_0/F
1.0
1.2
1.4
1.6
1.8
0
5
10
15
20
25
[AgNP], pM

Figure 4B

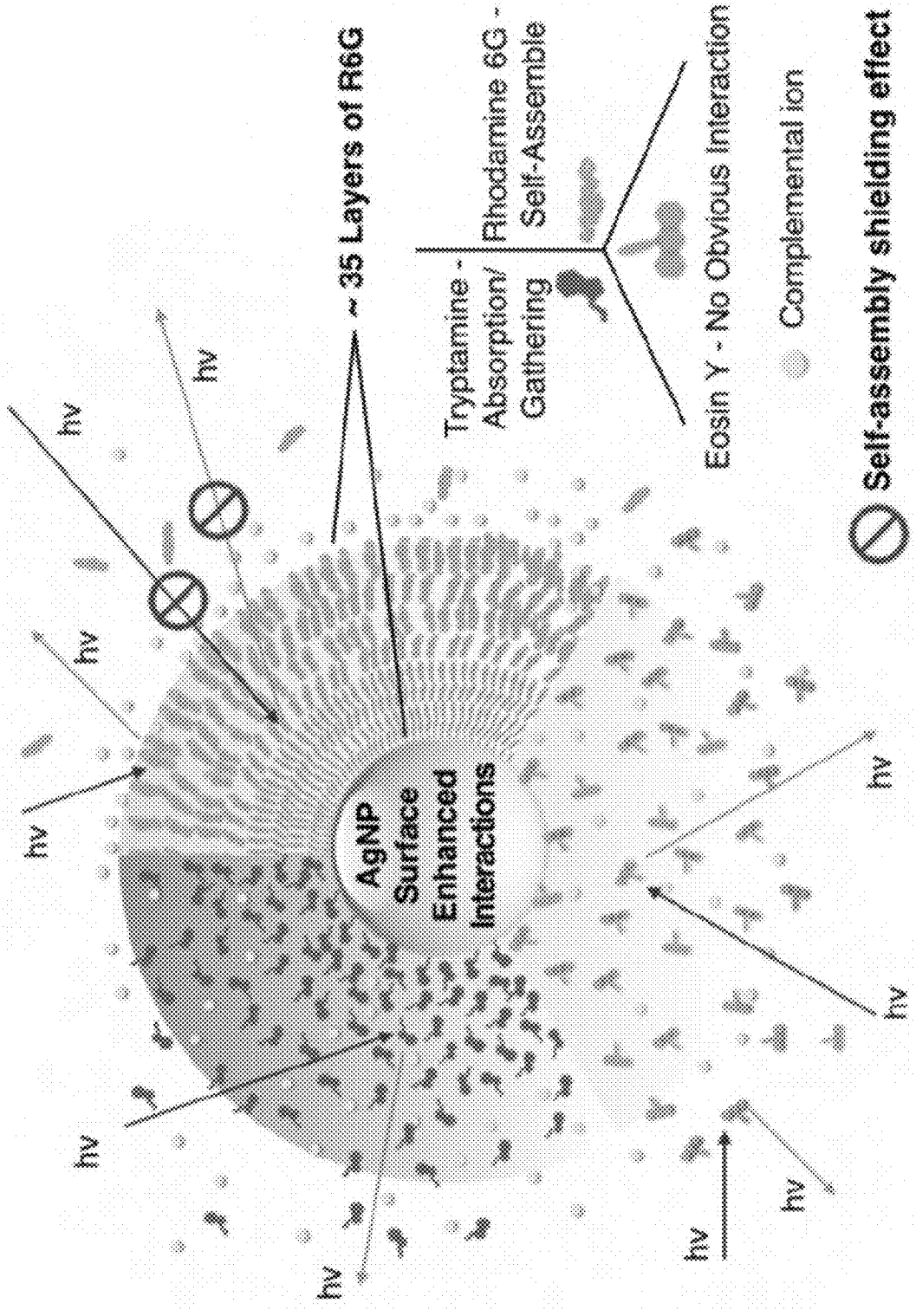
hv
~ 35 Layers of R6G
Tryptamine - Absorption/ Gathering
Rhodamine 6G - Self-Assemble
Eosin Y - No Obvious Interaction
Complemental ion
Self-assembly shielding effect
AgNP Surface Enhanced Interactions

Figure 5

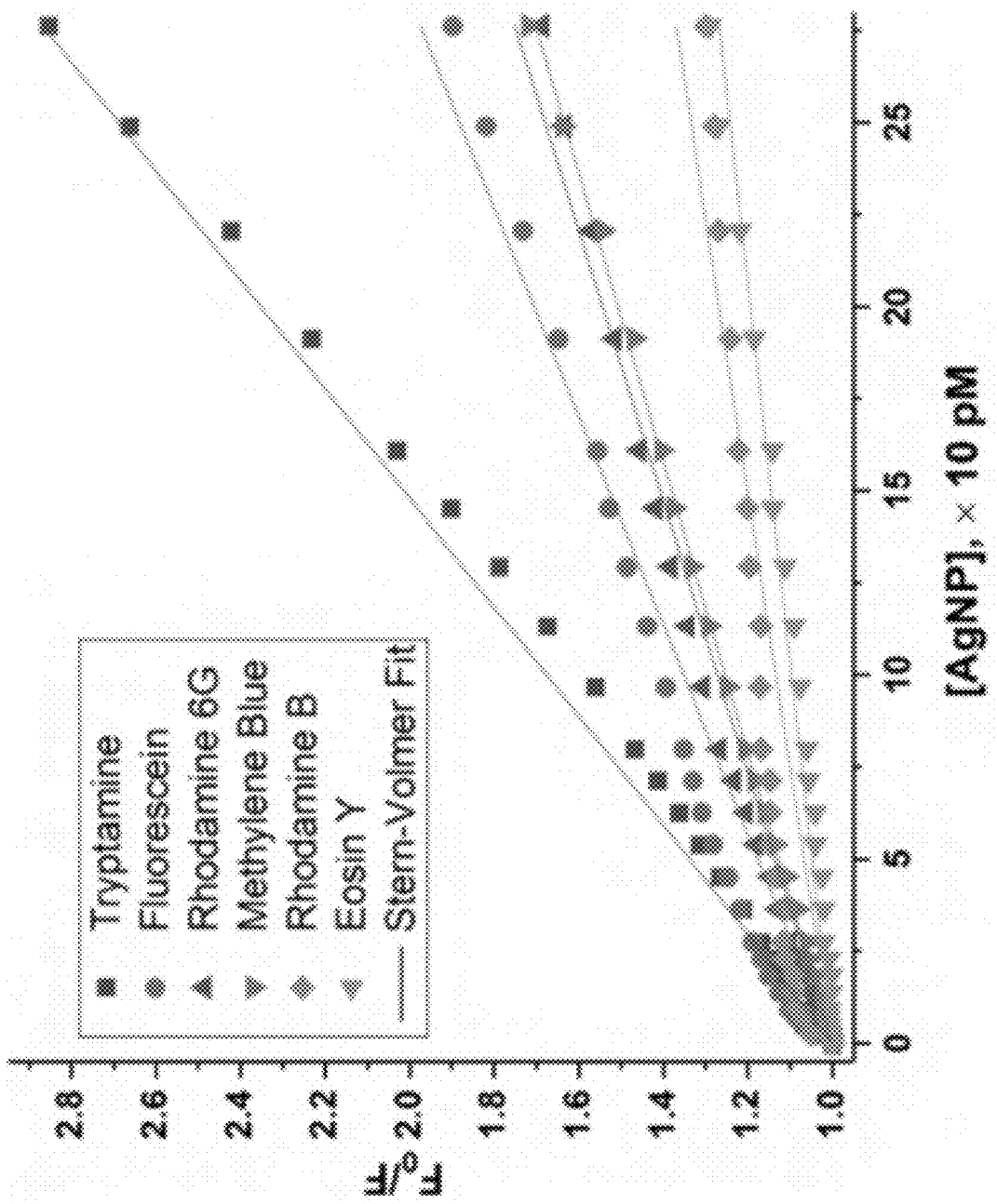
Tryptamine
Fluorescein
Rhodamine 6G
Methylene Blue
Rhodamine B
Eosin Y
Stern-Volmer Fit
F_0/F
[AgNP], × 10 pM
0
5
10
15
20
25
1.0
1.2
1.4
1.6
1.8
2.0
2.2
2.4
2.6
2.8

Figure 6

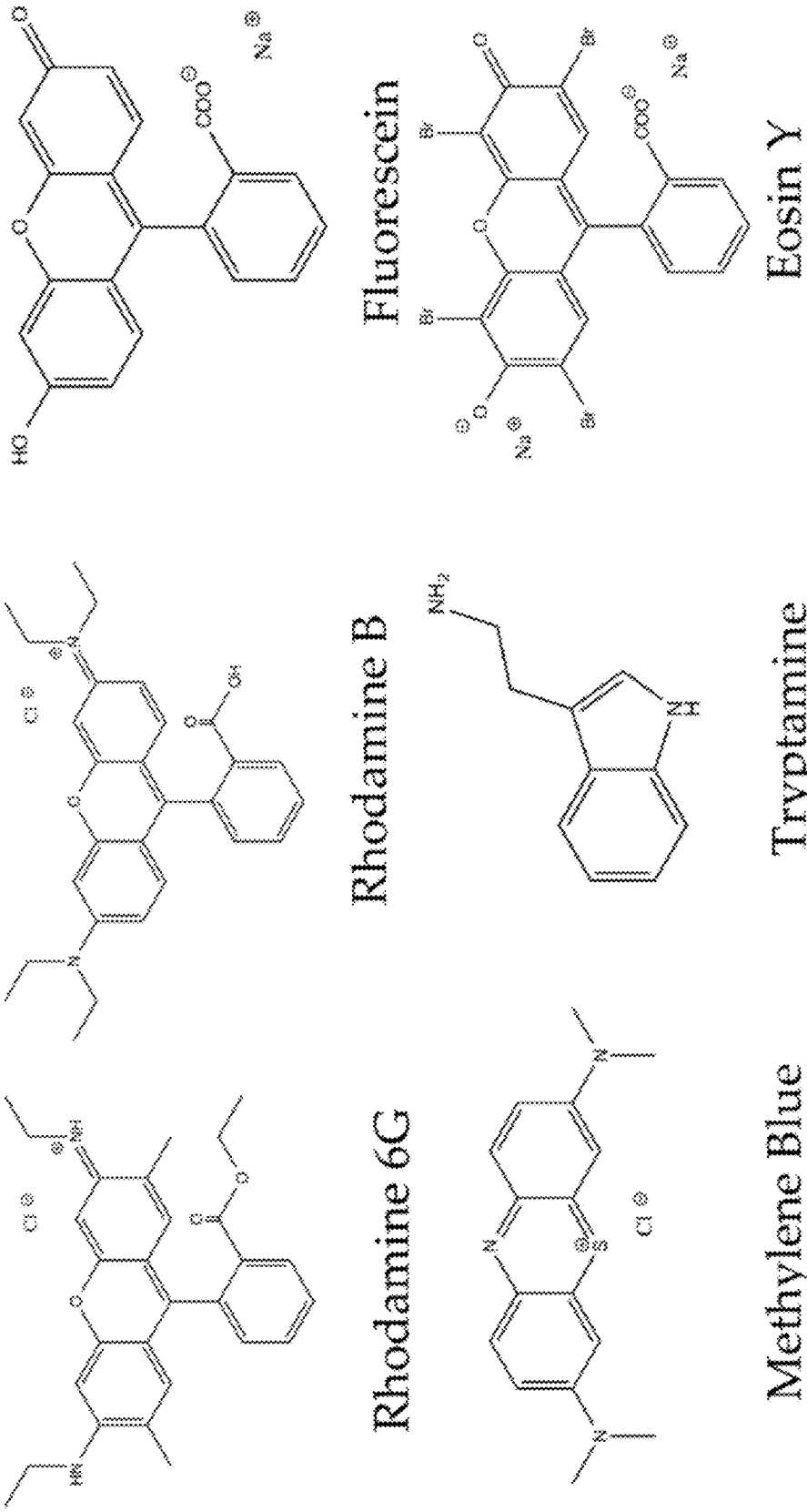
Fluorescein
Eosin Y
Rhodamine B
Tryptamine
Rhodamine 6G
Methylene Blue

Figure 7

SILVER NANOPARTICLE SURFACE ENABLED SELF-ASSEMBLY OF ORGANIC DYE MOLECULES

GOVERNMENT LICENSE RIGHTS

[0001] Portions of the invention described herein were made with government support from the United States Army Research Lab (W911NF-122-0022) and the National Science Foundation (Grant DMR-0611539). The U.S. government may have certain rights in the invention.

BACKGROUND OF THE INVENTION

[0002] Metal nanoparticles (NP) have shown great potential for use in catalysis [1], sensing [2], imaging [3,4] and antimicrobials [5,6]. Over 400 tons of silver nanoparticle (AgNP) have been produced annually and 30% of them are used in medical applications due to their antibacterial properties [7]. Most of these nanoparticle-containing products will be released to the environment and ultimately conduct unique interactions with biomolecules, such as the formation of protein and environmental corona [8,9]. These interactions are a result of the surface interactions between AgNP and ambient species or through surface-enabled molecular interactions. Hence, it is of interest to understand AgNP surface-enabled molecular interactions and reactions, which are also fundamental to the understanding of the toxicity of AgNP [10].

[0003] There have been reports on the study of the interaction between AgNP and biologically active small molecules such as dopamine [11], melamine [12], and pyronin Y [13], and organic molecules containing thiol groups [14]. In general, AgNPs have the highest binding affinity to thiol containing molecules [14,15]. Log K of —SR to Ag(I) is 12, compared to 2.1 and 3.4 for —OR and —NH groups, respectively [16]. Munro et al. [17] studied the surface of citrate-coated AgNP using surface-enhanced Raman spectroscopy (SERS), they suggested that citrate's two carboxylate groups bind the surface Ag atoms of the AgNP while its tertiary hydroxyl group forms intermolecular hydrogen bonds, and with the third carboxylate acting as a reaction site. Petty et al. [18] confirmed that cysteine moieties are the main sites for AgNP attachment in DNAs. Zhao et al. [19] reported that rhodamine 6G (R6G) molecules can form dimers on AgNP surface, which is related to localized surface plasmon resonance. These findings open some insights into the molecular interaction on the surface of AgNP.

[0004] Due to the lack of effective instruments or methods, it is difficult to obtain direct information on the interaction between AgNP and small molecules. To estimate the number of small molecules bound to AgNP, one has to go through a complex process: AgNP-organic molecule complexes are often separated from free organic molecules in solution using centrifugation, followed by mass spectroscopy or UV-vis spectrometry to examine the amount of organic molecules bound to AgNP surface. The number of molecules bound to each AgNP can be estimated by comparing the concentration differences of these molecules before and after mixing with AgNP [6,20,21]. X-ray structure was used to study the structure of the crystalized complex of a gold nanocluster (102 Au atoms) with p-mercaptobenzoic acid (p-MBA), which showed that 44 p-MBA molecules bind to 23 surface Au atoms [22]. The resolution was 1.1 Å. However, there have been no such studies for AgNP [23-25]. Currently, only surface plasmon resonance and SERS [12, 17] have been used to investigate AgNP interaction with small molecules, while theoretical calculations based on density functional theory or first principles quantum theory [12,26] complement the experimental studies.

SUMMARY OF THE INVENTION

[0005] We studied the interactions of RG6, rhodamine B, methylene blue, fluorescein, eosin Y and tryptamine with AgNP through fluorescence titration, a method also used to investigate interactions between proteins and metal NP [27,28], and discovered that RG6, rhodamine B and methylene blue self-assemble around a single AgNP to form micelles and micelle agglomerates.

[0006] Accordingly, there is presented according to an embodiment of the invention, a self-assembling nano-particle-based micelle composition, comprising a silver nanoparticle core and a plurality of layers of positively charged aromatic nitrogen-containing compounds. According to various alternative embodiments, the silver nanoparticle may be citrate-coated; the silver nanoparticle may be present in solution at a concentration of about 1 μM or less; the positively charged aromatic nitrogen-containing compounds may be present in solution at a concentration of about 1 μM or less; the positively charged aromatic nitrogen-containing compounds may be dye compounds, including but not limited to Rhodamine 6G, Rhodamine B, and Methylene Blue.

[0007] There is further presented according to an embodiment of the invention a method for preparing self-assembling nano-particle-based micelle composition, comprising a silver nanoparticle core and a plurality of layers of positively charged aromatic nitrogen-containing compounds, the method comprising gradually adding a 1 μM solution of silver nanoparticle to a 1 μM solution of positively charged aromatic nitrogen-containing compound. According to various embodiments of the invention, the silver nanoparticle may be citrate-coated; the silver nanoparticle may be present in solution at a concentration of about 1 μM or less; the positively charged aromatic nitrogen-containing compounds may be present in solution at a concentration of about 1 μM or less; the positively charged aromatic nitrogen-containing compounds may be dye compounds, including but not limited to Rhodamine 6G, Rhodamine B, and Methylene Blue.

[0008] There is also presented according to the invention, a method for aggregating positively charged aromatic nitrogen-containing compounds in solution, comprising adding silver nanoparticles to a solution containing said positively charged aromatic nitrogen-containing compounds. According to various embodiments of the invention, the silver nanoparticle may be citrate-coated; the silver nanoparticle may be present in solution at a concentration of about 1 μM or less; the positively charged aromatic nitrogen-containing compounds may be present in solution at a concentration of about 1 μM or less; the positively charged aromatic nitrogen-containing compounds may be dye compounds, including but not limited to Rhodamine 6G, Rhodamine B, and Methylene Blue.

BRIEF DESCRIPTION OF THE DRAWINGS

[0009] FIG. **1**A. Fluorescence quenching of 1 μM solution of R6G dye upon addition of various amounts of 240 pM AgNP.

[0010] FIG. **1**B. Fluorescence quenching of 1 μM solution of rhodamine B upon addition of various amounts of 240 pM AgNP.

[0011] FIG. **1**C. Fluorescence quenching of 1 μM solution of fluorescein upon addition of various amounts of 240 pM AgNP.

[0012] FIG. **1**D. Fluorescence quenching of 1 μM solution of tryptamine upon addition of various amounts of 240 pM AgNP.

[0013] FIG. **1**E. Fluorescence quenching of 1 μM solution of Methylene Blue upon addition of various amounts of 240 pM AgNP.

[0014] FIG. **1**F. Fluorescence quenching of 1 μM solution of eosin Y upon addition of various amounts of 240 pM AgNP. The insert shows the enlarged detail of fluorescence peaks, where comparatively weak quenching is observed.

[0015] FIG. **2**A. Plot of fluorescence intensity ratio (F_0/F) versus AgNP concentration at dye concentration of 1 μM. Average value from five measurements are shown and error bars are removed for a better comparison.

[0016] FIG. **2**B. Plot of fluorescence intensity ratio (F_0/F) versus AgNP concentration at dye concentration of 10 μM. Average value from five measurements are shown and error bars are removed for a better comparison.

[0017] FIG. **3**. Fit of F_0/F verse (AgNP) plot of eosin Y.

[0018] FIG. **4**A. Fit of F_0/F verse [AgNP] plot of 1 μM R6G, rhodamine B, and methylene blue.

[0019] FIG. **4**B. Fit of F_0/F verse [AgNP] plot of 1 μM fluorescein and tryptamine.

[0020] FIG. **5**. Schematic drawing of different types of interaction and behavior of various dye molecules, and "self-assembly shielding effect" caused by self-assemble of Rhodamine 6G molecules near AgNP surface.

[0021] FIG. **6**. Fit of F_0/F verse [AgNP] plot of dye molecules in the case of 10 μM. Error bars are removed for a better comparison.

[0022] FIG. **7**. Structures of tested dye molecules.

DETAILED DESCRIPTION

[0023] Silver nitrate, sodium borohydride, sodium citrate, R6G, rhodamine B, methylene blue, fluorescein, eosin Y, and tryptamine were purchased from Sigma Aldrich (St. Louis, Mo.). Nitric acid (trace metal grade, 67-70%) was from Fisher Scientific (Houston, Tex.).

[0024] AgNPs were prepared following a previous reported method [6,29] using sodium borohydride to reduce silver nitrate, followed by citrate mediated reduction and growth [30,31]. Briefly, silver nitrate (17 mg) and sodium borohydride (15 mg) were each dissolved in 90 mL ice-chilled nanopure water. The two solutions were mixed slowly, and a yellowish color appeared. The mixture was left for 5 min under stirring followed by addition of 10 mL of sodium citrate (70 mg). The resultant solution was heated and kept under reflux at 90-95° C. for 30 min. After cooling to room temperature, the solution was centrifuged at 5000 rpm for 1 h and the pellet was collected and suspended into 20 mL water. Centrifugation was repeated twice to remove extra reactants. Finally, a further centrifugation at 2000 rpm for 30 min to remove the largest NPs was carried out and the supernatant was collected and kept in the refrigerator as AgNP stock solutions for further experiments.

[0025] The AgNP was characterized by UV-vis spectroscopy (UV-2600 spectrophotometer, Shimadzu, Kyoto, Japan) and Transmission Electron Microscopy (TEM, JOEL 2100, Tokyo, Japan). AgNPs have a characteristic extinction peak at 398 nm. The TEM images show that citrate-coated AgNPs have spherical morphology of an average diameter of 24±7 nm.

[0026] To determine the concentration of AgNP, its solution was added with nitric acid to completely oxidize all Ag atoms to Ag^+ ions. The resultant Ag^+ solution was diluted with nanopure water until the estimated Ag^+ concentration ranged from 20 to 100 ppb. It was then analyzed by ICP-MS (Varian 820-MS, Palo Alto, USA) to determine the total concentration of Ag^+ ion and thus the concentration of the AgNP in terms of Ag atoms.

[0027] The number of Ag atoms in each AgNP was estimated by the following equation [33,33],

$$N = \frac{\pi}{6}\frac{\rho d^3}{M}N_A = \frac{\pi N_A d^3}{6V_m} = 30.67d^3 \quad (1)$$

where ρ is the density of Ag (10.49 g/cm^3), M is the atomic weight of Ag (107.87 g/mol), V_m is molar volume (10.5 mL mol^{-1}), d is the diameter of AgNP in nm. It yields 420,000 Ag atoms per one 24 nm AgNP. Therefore, the concentrations in terms of Ag atoms that are obtained from ICP-MS can be converted to concentrations in terms of AgNP. E.g., 100 μM in term of Ag atoms equals to 2.4×10^{-4} μM or 240 pM in term of AgNP. Concentrations used below are in terms of AgNP.

[0028] Two concentrations of dye molecules, 1 μM and 10 mM, were used for fluorescence titrations. Fluorescence parameter of different dyes and instrumental setup are shown in Table 1. AgNP (240 pM or 2400 pM) were titrated into 2,000 μL of dye solutions of 1 μM and 10 μM, respectively, with the following volumes of 0, 2.5, 2.5, 2.5, 2.5, 5.0, 5.0, 5.0, 5.0, 10.0, 10.0, 10.0, 10.0, 10.0, 10.0, 20.0, 20.0, 20.0, 20.0, 20.0, 40.0, 40.0, 40.0, and 40.0 μL. Emission spectra were recorded and fluorescence intensity values at the peak were collected and analyzed, using Fluoromax-4 spectrofluorometer (Horiba Scientific, Kyoto, Japan). The excitation spectra were also monitored upon addition of AgNP, following the same volume.

TABLE 1

Parameter and instrumental setup for fluorescence titrations.

Dye	Excitation Wavelength, nm	Slit Width, nm, 1 μm	Slit Width, nm, 10 μM	Emission Peak, nm
Rhodamine 6G	500	1	1	554
Rhodamine B	540	2	1	580
Methylene Blue	640	5	4	688
Fluorescein	470	1	1	513
Eosin Y	505	2	1	539
Tryptamine	280	2	2	356

[0029] When AgNP solutions are gradually added into the 1 μM or 10 μM dye solutions, it causes dilution to the original dye solution and thus lower the fluorescence intensity. The dilution factor, d_f, was used to correct the fluorescence intensity before the plot of fluorescence quenching curve, following Equations (2) and (3).

$$d_f = \frac{2000 + \Sigma_0^n V_i}{2000} \quad (2)$$

$$F_{actual} = F_{observed} \times d_f \quad (3)$$

[0030] V_i is the volume of AgNP solution added each time in the unit of μL, df is the dilution factor. F_{actual} and $F_{observed}$ are fluorescence intensities used for analysis and collected from fluorometer, respectively. Factual is the true fluorescence and used as F in the further analysis. Concentration of Ag^+ ions released from AgNP is very low (around 100 nM level) [6] and their quenching to R6G fluorescence is less than 1% [34]. This is confirmed by using $AgNO_3$ solution of equivalent concentration as a control quencher and it shows no effect on fluorescence of dye molecules. Therefore, the role of Ag^+ ions on fluorescence quenching is ignored in the current study.

[0031] DLS was employed to monitor the change of dynamic size and zeta-potential during titrations, using a Zetasizer Nano-ZS (Malvern, UK).

[0032] Effect of AGNPs on the Fluorescence of Dye Molecules

[0033] Fluorescence spectra of 1 μM dye solutions upon addition of various amounts of the 240 pM AgNP solutions are shown in FIGS. **1**A-**1**F. As AgNP solutions are gradually added to the solution of the dyes, the fluorescence intensity of the dyes decreases, an indication of quenching, although the rates of fluorescence decrease are different for different dyes. The emission spectra for all the dyes remain the same during titration except tryptamine, whose emission maximum shifts to a shorter wavelength from 359 to 356 nm. The titration into the 10 μM dye solutions also show similar fluorescence quenching patterns (data not shown) except that emission peak of tryptamine has a larger shift from 359 nm to 345 nm.

[0034] The effect of the addition of AgNP on fluorescence of various dye molecules in solution is analyzed by the Stern-Volmer plot, or plotting the fluorescence intensity ratio (F_0/F) versus AgNP concentration. The AgNP concentration on the x-axis of titration for the 10 μM dye solutions is also 10 times higher than that of the 1 μM dye solution (FIGS. **2**A and **2**B). The higher the F_0/F ratio, the more fluorescence is quenched.

[0035] In the case of 1 μM dye solution, the F_0/F of methylene blue, RG6 and rhodamine B increases sharply at the initial stage followed by a distinct turn for a slower increase at the AgNP concentration around 1-2 pM, indicating that R6G, methylene blue and rhodamine B molecules self-assemble on the surface of a single AgNP under these conditions to form micelles. As for eosin Y, the fluorescence quenching is at the very minimum. The plot for tryptamine and fluorescein, whose fluorescence ratios increase slowly, but steadily. Ultimately, they reach the highest quenching among all dyes tested.

[0036] When the concentration of the dye molecules is 10 the fluorescence of all dye molecules in solution is also quenched, without the sharp turn on the plots for R6G, methylene blue and rhodamine B observed when the dye solution is 1 μM. This indicates that the micelle-like self-assembly of these dye molecules on AgNP surface does not occur when the dye solution is at 10 μM. Fluorescein and tryptamine exhibit a much smoother quenching curve, which is also distinct with those of 1 μM dye solution. Eosin Y shows similar pattern since its quenching is weak.

[0037] Both absorption and excitation spectra were obtained for the titration. Due to low sensitivity of the photospectrometer, the absorption has to be done at 20 μM (or above) of the dye molecules. When 2400 pM of AgNP solution were titrated into 50 μM dye solution, R6G and methylene blue cause AgNP aggregation, while tryptamine, rhodamine B, fluorescein and eosin Y do not. In terms of absorption intensity, tryptamine, rhodamine B, fluorescein and eosin Y do not exhibit obvious decrease. The excitation spectra showed no shifts for all dye molecules.

[0038] Different Behaviors of the Dyes on AgNP Surface

[0039] Methylene blue, RG6 and rhodamine B as 1 μM solutions show similar quenching behaviors, with a sharp quenching at initial additions of AgNP until a sharp turn, followed by a much slower quenching. This demonstrates that methylene blue, RG6 and rhodamine B have the same capability to self-assemble on the AgNP surface to form stable micelle-like structures.

[0040] Fluorescence of fluorescein or tryptamine is gradually quenched with a smaller slope compared with R6G, rhodamine B and methylene blue, but lacks the "turn." These results indicate that fluorescein and tryptamine may gather around AgNP core in an absorption/tight interaction mode in a dynamic equilibrium but no stable micelle-like structure is formed since no obvious turn is observed (FIGS. **2**A and **2**B).

[0041] Eosin Y maintains a small but stable quenching slope during the whole titration.

[0042] These three types of molecular behaviors are further confirmed by the change of dynamic size and zeta-potential (Table 2). Rhodamine 6G and Rhodamine B have steady but dramatic change of both diameter and zeta-potential. Fluorescein and tryptamine have relative small size change with a difference around 34 nm and 36 nm, respectively. Size of AgNP in the presence of eosin Y is slightly increased due to "pre-concentration" that is further discussed below. Based on these interaction patterns, two mathematical models are used to fit the plot of F_0/F versus [AgNP] using Origin 2017 SR2.

TABLE 2

Dynamic diameter and zeta-potential of AgNP coated by citrate and in presence of six dye molecules.

	AgNP with citrate	Rhodamine 6G	Rhodamine B	Methylene Blue *	Fluorescein	EosinY	Tryptamine
Size, nm	33.4 ± 1.6	318.5 ± 34.4	197.6 ± 62.1	/	67.1 ± 12.4	42.8 ± 3.9	69.2 ± 13.0
Potential, mV	−47.3 ± 1.2	21.5 ± 2.0	17.6 ± 1.8	/	−16.9 ± 2.2	−31.8 ± 1.6	8.9 ± 3.7

Notes:

Data at the titration point of 2 pM AgNP is shown. At this point, the corresponding dye reach equilibrium between stable micelle-like structures or complexes and free molecules in solution.

* DLS results of methylene blue are not available due to interference between laser source wavelength of DLS (633 nm) and absorption of methylene blue (peaked at 612 nm and 664 nm).

[0043] Stern-Volmer Fluorescence Quenching Model for Eosin Y

[0044] For eosin Y, its fluorescence-quenching plot, F_0/F verse [AgNP], fits very well to the Stern-Volmer equation (FIG. **3**), with K_{sv} of 6.4 nM^{-1} of [AgNP], or 15,000 M^{-1} of [Ag] based on the estimate that one AgNP of 24 nm has about 420,000 Ag atoms.

[0045] Considering the Stern-Volmer equation,

$$\frac{F_0}{F} = 1 + k_q \tau_0 [AgNP] \tag{4}$$

the quenching rate constant k_q is comprised of two terms, the fraction of collisions that result in quenching f_Q, and the diffusion controlled bimolecular rate constant k_0.

$$k_q = f_Q k_o \tag{5}$$

$$k_0 = \frac{4\pi N_0}{1000\frac{\text{cm}^3}{\text{L}}}(r_f + r_q)(D_f + D_q) \tag{6}$$

where N_0 is Avogadro's number, r_f and r_q are the radii of the fluorophore and quencher, and D_f and D_q are the diffusion coefficients of the fluorophore and quencher, respectively. Based on the Stokes-Einstein equation

$$D = \frac{K_B \times T}{6\pi\eta r} \tag{7}$$

where K_B is Boltzmann constant, T is absolute temperature, η is the dynamic viscosity and r is the particle size. Diffusion coefficient (D) is mainly dependent on the particle size. Under current experimental conditions, eosin Y has a much smaller size than AgNP whose diffusion coefficient can be ignored when compared to that of eosin Y. Thus, Equation (4) can be rewritten as:

$$\frac{F_0}{F} = 1 + f_Q \tau_0 D_f \frac{4\pi N_0}{1000\frac{\text{cm}^3}{\text{L}}}(r_f + r_q)(AgNP) \tag{8}$$

[0046] Eosin Y has lifetime τ_0 of 2.50 ns [35] and small organic dye molecules normally have diffusion coefficients D_f around 420 μm^2 s^{-1} [36]. Given approximate radius of eosin Y and AgNP as 0.8 nm and 12.0 nm, equation [8] yields an f_Q of 6.17×10^{-20}, demonstrating an extremely low percentage of collisions that cause fluorescence quenching.

[0047] In contrast, eosin Y has an extremely high K_{sv} of 6.4 nM^{-1} of [AgNP], or 15,000 M^{-1} of [Ag], compared with the normal small molecule quenching, like the fluorescence quenching of tryptamine by acrylamide in an aqueous solution, which is around 33 M^{-1} [37]. Thus, the terms of traditional dynamic/collisional quenching and static quenching are not proper to describe fluorescence quenching by nanoparticles. Instead, we employed "nanoparticle surface enabled fluorescence quenching" to describe fluorescence quenching of eosin Y by AgNP.

[0048] Mathematics Model for the Molecular Self-Assembly on AgNP Surface

[0049] Plots of F_0/F of rhodamine B, R6G, and methylene blue versus [AgNP] all fit very well to a function composed of an exponential term (self-assembly shielding effect) plus a Stern-Volmer term (nanoparticle surface enhanced fluorescence quenching), shown in FIGS. **4**A and **4**B and Equation (9).

$$\frac{F_0}{F} = A(1 - e^{-\frac{(AgNP)}{B}}) + (1 + K_{SV}(AgNP)) \tag{9}$$

[0050] The resulting constants A, B, and K_{sv} are listed in Table 2 from the excellent fits.

[0051] The initial exponential term represents the rapid quenching through self-assembly shielding effect, where the internal dye molecules of the micelles cannot absorb light and thus not get to the excited state to fluoresce, due to the self-assembly of the dye molecules on the surface of AgNP. Constant A corresponds to the AgNP concentration at which a stable micelle-like structure is in an equilibrium with the free dye molecules in solution. The higher is the A value, the lower is the concentration required for the corresponding dye to reach equilibrium between stable micelle-like structures and those free in solution. Thus, three dyes that form stable micelle-like structures follow a formation sequence from fastest to lowest: methylene blue>R6G>rhodamine B (A values of 0.33, 0.20 and 0.16, respectively).

[0052] Constant B represents the relative binding affinity between AgNP and dye molecules. Smaller B values indicate stronger interactions, and larger numbers of dye molecules gathering around each AgNP at equilibrium, and ultimately self-assembly shielding effect as well as fluorescence quenching percentages. The three dyes follow an interaction affinity sequence of rhodamine B<methylene blue<R6G (B values of 0.59, 0.38 and 0.33, respectively).

[0053] The fluorescence quenching of R6G, rhodamine B and methylene blue by AgNP have an obvious turning point where stable "micelle"-like structures are formed. Equation (5) is employed to estimate the number of dye molecules that assemble on the surface of each AgNP, assuming that all the fluorescence quenching is caused by interactions between dye molecules and the AgNP.

$$\frac{\text{Quenched Dye}}{AgNP} = \frac{2000\ \mu\text{L}\times 1\ \mu\text{M}\times N_0 \frac{I}{I_0}}{240\ pM \times N_0 \Sigma_0^N V_i} = \frac{10^8 \times \frac{I}{I_0}}{12 \times \Sigma_0^n V_i} \tag{10}$$

[0054] V_i is the value of each titration volume, with unit of μL. At the turning point, this ratio demonstrates the number of molecules in a single stable micelle-like structure, in other words, the number of dye molecules that a stable "micelle" can "hold" in a dynamic equilibrium. The estimated numbers are listed in Table 3, with 180,000, 200,000, and 220,000 for rhodamine B, methylene blue, and R6G, respectively, per AgNP. This number indicates that at dynamic equilibrium, the majority of the dye molecules in solution are assembled on AgNP. The remaining small portion is close to the "minimum" concentration of free dye molecules to maintain balance in the solution.

[0055] The Stern-Volmer term K_{sv}, representing the collisional quenching, has values for rhodamine B, R6G, and methylene blue of 5.5, 8.9 and 10 nM^{-1} of [AgNP], respectively, or 13,000, 21,000, and 24,000 M^{-1} of Ag atoms.

[0056] The fluorescence quenching graphs for tryptamine and fluorescein also fit to Equation (9), but due to the lack of the sharp turn, there is no indication of a definitive "micelle" formed. Therefore, there is no estimate made for the number of molecules per AgNP. The fitting parameters A, B, and K_{sv} are on the same order of magnitude with those for methylene blue, rhodamine B and R6G, but the parameters B and K_{sv} values are obviously larger (Table 3). This demonstrates an absorption/tight interaction mode on AgNP surface and "pseudo-micelles" could be formed with these dyes (FIG. **5**).

TABLE 3

Mathematical fitting results for all dye molecules.

$$\frac{?}{F} = A(1 - ?) + (1 + K_{sv}[AgNP])$$

Dye	A	B	K_{sv}, nM^{-1} (AgNP)	K_{sv}, M^{-1} (Ag)	R^2	Dyes/ AgNP
Rhodamine B	0.16	0.59	5.5	13,000	0.992	180,000
Rhodamine 6G	0.20	0.33	8.9	21,000	0.996	220,000
Methylene Blue	0.33	0.38	10	24,000	0.995	200,000
Fluorescein	0.37	3.37	1.5	36,000	0.998	/
Tryptamine	0.12	1.27	1.8	43,000	0.999	/
Eosin Y	/	/	6.4	15,000	0.997	/
Tryptamine*	/	/	/	33*	/	/

*The K_{sv} for triptamine quenching by acrylamide is 33 M^{-1} [38].

? indicates text missing or illegiblewhen filed

[0057] "Super" Stern-Volmer Fluorescence Quenching Constant

[0058] One interesting observation is that the Stern-Volmer quenching constant (nanoparticle surface enhanced fluorescence quenching) for all the six dye molecules assembled on AgNP are generally three orders of magnitude higher than the normal small molecule quenching, like the fluorescence quenching of tryptamine by acrylamide in an aqueous solution, which is around 33 M^{-1} [37], making AgNP a super-quencher [38]. One explanation is that the dye molecules, except those forming the micelles, are in close proximity of AgNP, or "pre-concentrated" on the AgNP surface. During this process, fluorescence quenching is a complicated result caused by a combined self-assembly shielding effect and traditional static and even dynamic quenching. This again indicates that these dye molecules, charged or neutral, are in the proximity of the AgNP.

[0059] "Self-Assembly Shielding Effect" Caused Fluorescence Quenching

[0060] It is well known that aggregation, including self-assembly, causes fluorescence quenching of dye molecules in aqueous solution (it is sometimes termed "aggregation caused fluorescence quenching, ACQ"), owing to electron or energy transfer [39-41]. It occurs under relatively high concentrations for aggregation, at 10 μM or higher [42,43]. In our case, the self-assembly of dye molecules on AgNP surface indicates that traditional electron or energy transfer (among dye molecules) causes fluorescence quenching, even under 1 μM for both the dye and AgNP. However, it cannot explain the "sharp turn" of the plot for R6G, methylene blue and rhodamine B.

[0061] Taking R6G as an example, 210,000 R6G molecules assemble on a single AgNP (24 nm) with an estimated 35 layers. As shown in FIG. **5**, the inner layers of R6G would be shielded from absorbing light and fluoresce [43], termed "self-assembly shielding effect" to describe the unique fluorescence quenching caused by self-assembly of dye molecules on AgNP surface. Considering that 35 layers of dye molecules, R6G, methylene blue or rhodamine B are tightly surrounding the AgNP core, the excitation light could penetrate approximately the outmost one to several layers (due to gaps among dye molecules). It cannot travel through many layers of self-assembled dye molecules to reach those of inner layers. Therefore, inner layers of dye molecules are shielded from excitation by light and thus would not generate any fluorescence. This is a unique fluorescence quenching mechanism caused by AgNP enabled self-assembly behavior, with a characteristic "sharp turn" on the plot of fluorescence intensity ratio (F_0/F) versus AgNP concentration (FIGS. **2**A and **2**B).

[0062] For dye molecules that have loose or no obvious interaction with AgNPs, like eosin Y in FIG. **3**, the pathway of light is not completely blocked so that its fluorescence quenching is mainly caused by electron transfer, Førster resonance energy transfer (FRET) and/or nanosurface energy transfer (NSET). Some organic molecules show a fluorescence quenching efficiency between R6G and eosin Y, indicating they have a gathering around AgNP but it is not as dense/thick, nor as well-organized as that of R6G. Self-assembly shielding effect may also be involved but it is not that obvious.

[0063] Factors Affecting Molecular Interactions on AgNP Interface

[0064] Concentration of both Dyes and Nanoparticles

[0065] It is obvious that the self-assembly of dye molecules on AgNP surface is concentration dependent; and it only occurs at low concentrations for both AgNP and dyes. For the dye solutions of 10 all quenching plots fit to a pseudo Stern-Volmer plot (FIG. **6**) with K_{sv} values of 10-68 nM^{-1} [AgNP] (Table 4), higher than those constants for dyes in the 1 μM solutions. Such large Stern-Volmer quenching constants still indicate super-quenching. At the [AgNP]/[dye] ratio of 30, the quenching strength from the most to the least quenched dyes are: fluorescein>tryptamine methylene blue>rhodamine 6G>rhodamine B>eison Y for 1 μM dye solutions; and tryptamine>fluorescein>methylene blue rhodamine 6G>rhodamine B≤eison Y for 10 μM dye solutions. It is obvious that concentration plays an important role on fluorescence quenching by AgNP.

TABLE 4

Stern-Volmer fit results (K_{sv} in nM^{-1} of [AgNP]) with the concentration of the dyes at 10 μM.

	Tryptamine	Fluorescein	R6G	Methylene Blue	Rhodamine B	Eosin Y
K_{sv}	68	35	27	25	13	10

[0066] Intrinsic Molecular Structure

[0067] The structures of all tested dyes are shown in FIG. **7** and their properties are listed in Table 5 with information

on charge, functional groups and paired ions. Self-assembly is determined from interactions between AgNP and dye molecules at 1 μM as shown in FIGS. **2**A and **2**B.

TABLE 5

Properties of dye molecules and their fluorescence quenching behavior.

Dye	Charge	Functional Groups	Pair Ions	Self-Assembly
Rhodamine 6G	1+	—NH—, —N═, —O—, —COO—	Cl^-	Yes
Rhodamine B	1+	—N—, —N═, —O—, —COO—	Cl^-	Yes
Methylene Blue	1+	—N—, —N═, —S—	Cl^-	Yes
Fluorescein	1−	—OH, —COO—, —O—, ═O	Na^+	Weak
Eosin Y	2−	—COO—, —Br—, —O—, ═O	Na^+	No
Tryptamine	0	—NH—, $—NH_2$	NA	Weak

[0068] Charge

[0069] All dye molecules forming the micelle-like self-assemblies on AgNP have a positive charge, indicating positive charge promotes the self-assembly of the dyes on AgNP. Surface of citrate-coated AgNP are negatively charged, thus AgNP favors binding to positively charged molecules. It is rather unusual that these positively charged aromatic dye molecules self-assemble on the AgNP surface to form large micelles.

[0070] Functional Groups

[0071] In addition to the positive charge, rhodamine B, R6G and methylene blue all have some nitrogen atoms in the molecule. We think that the nitrogen group also helps to facilitate the micelle formation. The other feature of these three molecules are the relatively large and flat aromatic moieties, which might be necessary for the micelle formation. However, it is difficult to pinpoint the exact roles the functional groups play in the self-assembly, as well as the "pre-concentration" on the AgNP surface. These results are in agreement with previous reports that AgNP have preferable binding sites in terms of specific functional groups and other protein components or secondary structure [12,15,44, 45]

CONCLUSIONS

[0072] Furthermore, the self-assembly can only occur at low concentrations (at 1 μM or lower) for both dye and AgNP, while at a higher dye concentration (10 μM) yields pseudo Stern-Volmer quenching curves. Although the quenching of fluorescein and tryptamine by AgNP also fits to the same two-term model, the quenching curve lacks the signature "sharp turn" for the formation of the "micelle-like" self-assembly. The quenching of eosin Y follows the Stern-Volmer quenching model very well without the exponential term. The Stern-Volmer quenching constants (K_{sv}) for these dyes are in the range of 1.5-10 nM^{-1} of [AgNP], or 13,000-43,000 M^{-1} of [Ag], three orders of magnitude higher than the value of the collisional quenching of tryptamine fluorescence by acrylamide (33 M^{-1}).

[0073] Such a "super-quenching" by AgNP can only be attributed to "pre-concentration" of the dye molecules on the nanoparticle surface. The "pre-concentration" of methylene blue/R6G/rhodamine B near the surface of AgNP further yields the formation of micelle-like self-assembly, resulting in even greater fluorescence quenching during the initial stage of the titration. Detailed mechanisms of self-assembly remain to be explored but the common features of all these dye molecules are the positive charge, the aromatic moiety, and the polar groups. The charge of the dye molecules seems to be the dominant factor. Negatively charged or neutral molecules are not likely to self-assemble on the AgNP surface. The fluorescence quenching for Methylene Blue, Rhodamine B, and R6G all fit to a mathematical model with an exponential term (self-assembly) and a Stern-Volmer term (nanoparticle surface enhanced quenching).

[0074] These findings and models provide fundamental information of nanoparticle surface enabled interaction and molecular behavior, which could further facilitate the understanding of protein and environmental corona formation, and benefit engineering nanoparticle-based nanomaterials.

[0075] Having now fully set forth the preferred embodiments and certain modifications of the concepts underlying the present invention, various other embodiments as well as certain variations and modifications of the embodiments herein shown and described will obviously occur to those skilled in the art upon becoming familiar with said underlying concepts. If should be understood, therefore, that the invention may be practiced in ways other than explicitly set forth herein and still fall entirely within the scope of the present invention.

REFERENCES

[0076] 1. Zhang, W.; Lu, G.; Cui, C.; Liu, Y.; Li, S.; Yan, W.; Xing, C.; Chi, Y. R.; Yang, Y.; Huo, F. A Family of Metal-Organic Frameworks Exhibiting Size-Selective Catalysis with Encapsulated Noble-Metal Nanoparticles. *Adv. Mater.* 2014, 26, 4056-4060

[0077] 2. Howes, P. D.; Chandrawati, R.; Stevens, M. M. Colloidal nanoparticles as advanced biological sensors. *Science* 2014, 346, 1247390.

[0078] 3. Lee, N.; Yoo, D.; Ling, D.; Cho, M. H.; Hyeon, T.; Cheon, J. Iron Oxide Based Nanoparticles for Multimodal Imaging and Magnetoresponsive Therapy. *Chem. Rev.* 2015, 115, 10637-10689.

[0079] 4. Jiang, S.; Win, K. Y.; Liu, S.; Teng, C. P.; Zheng, Y.; Han, M.-Y. Surface-functionalized nanoparticles for biosensing and imaging-guided therapeutics. *Nanoscale* 2013, 5, 3127-3148.

[0080] 5. Zhang, Y.; Dasari, T. P. S.; Deng, H.; Yu, H. Antimicrobial Activity of Gold Nanoparticles and Ionic Gold. *J. Environ. Sci. Health Part C* 2015, 33, 286-327.

[0081] 6. Deng, H.; McShan, D.; Zhang, Y.; Sinha, S. S.; Arslan, Z.; Ray, P. C.; Yu, H. Mechanistic study of the synergistic antibacterial activity of combined silver nanoparticles and common antibiotics. Environ. Sci. Technol. 2016, 50, 8840-8848.

[0082] 7. Pourzahedi, L.; Eckelman, M. J. Environmental life cycle assessment of nanosilver-enabled bandages. Environ. Sci. Technol. 2014, 49, 361-368.

[0083] 8. Chen, F.; Wang, G.; Griffin, J. I.; Brenneman, B.; Banda, N. K.; Holers, V. M.; Backos, D. S.; Wu, L.; Moghimi, S. M.; Simberg, D. Complement proteins bind to nanoparticle protein corona and undergo dynamic exchange in vivo. Nat. Nanotech. 2017, 12, 387-393.

[0084] 9. Pulido-Reyes, G.; Leganes, F.; Fernandez-Piñas, F.; Rosal, R. Bio-nano interface and environment: A critical review. Environ. Toxicol. Chem. 2017, 36, 3181-3193.

[0085] 10. Deng, H.; Zhang, Y.; Yu, H. Nanoparticles considered as mixtures for toxicological research. J. Environ. Sci. Health Part C 2018, 36, 1-20.

[0086] 11. Liu, C.; He, H.; Pandey, R.; Hussain, S.; Karna, S. P. Interaction of Metallic Nanoparticles with a Biologically Active Molecule, Dopamine. J. Phys. Chem. B 2008, 112, 15256-15259.

[0087] 12. Chen, X.; Hu, Y.; Gao, J.; Zhang, Y.; Li, S. Interaction of Melamine Molecules with Silver Nanoparticles Explored by Surface-Enhanced Raman Scattering and Density Functional Theory Calculations. Appl. Spectrosc. 2013, 67, 491-497.

[0088] 13. Senol, A. M.; Metin, Ö.; Acar, M.; Onganer, Y.; Meral, K. The interaction of fluorescent Pyronin Y molecules with monodisperse silver nanoparticles in chloroform. J. Mol. Struct. 2016, 1103, 212-216.

[0089] 14. Choi, S.-H.; Lee, S.-H.; Hwang, Y.-M.; Lee, K.-P.; Kang, H.-D. Interaction between the surface of the silver nanoparticles prepared by γ-irradiation and organic molecules containing thiol group. Radiat. Phys. Chem. 2003, 67, 517-521.

[0090] 15. Deng, H.; Yu, H. A mini review on controlling the size of Ag nanoclusters by changing the stabilizer to Ag ratio and by changing DNA sequence. Adv. Nat. Sci. 2015, 8, 1-9.

[0091] 16. Smith, D. S.; Bell, R. A.; Kramer, J. R. Metal speciation in natural waters with emphasis on reduced sulfur groups as strong metal binding sites. Comp. Biochem. Physiol. C Toxicol. Pharmacol. 2002, 133, 65-74.

[0092] 17. Munro, C. H.; Smith, W. E.; Garner, M.; Clarkson, J.; White, P. C. Characterization of the Surface of a Citrate-Reduced Colloid Optimized for Use as a Substrate for Surface-Enhanced Resonance Raman Scattering. Langmuir 1995, 11, 3712-3720.

[0093] 18. Petty, J. T.; Zheng, J.; Hud, N. V.; Dickson, R. M. DNA-Templated Ag Nanocluster Formation. J. Am. Chem. Soc. 2004, 126, 5207-5212.

[0094] 19. Zhao, J.; Jensen, L.; Sung, J.; Zou, S.; Schatz, G. C.; Van Duyne, R. P. Interaction of Plasmon and Molecular Resonances for Rhodamine 6G Adsorbed on Silver Nanoparticles. J. Am. Chem. Soc. 2007, 129, 7647-7656.

[0095] 20. Basheer, N. S.; Kumar, B. R.; Kurian, A.; George, S. D. Thermal lens probing of distant dependent fluorescence quenching of Rhodamine 6G by silver nanoparticles. J. Lumin. 2013, 137, 225-229.

[0096] 21. Tom, R. T.; Pradeep, T. Interaction of azide ion with hemin and cytochrome c immobilized on Au and Ag nanoparticles. Langmuir 2005, 21, 11896-11902.

[0097] 22. Jadzinsky, P. D.; Calero, G.; Ackerson, C. J.; Bushnell, D. A.; Kornberg, R. D. Structure of a Thiol Monolayer-Protected Gold Nanoparticle at 1.1 A Resolution. Science 2007, 318, 430-433.

[0098] 23. Pollard, T. D. A guide to simple and informative binding assays. Mol. Biol. Cell 2010, 21, 4061-4067.

[0099] 24. Richter, A. P.; Brown, J. S.; Bharti, B.; Wang, A.; Gangwal, S.; Houck, K.; Hubal, E. A. C.; Paunov, V. N.; Stoyanov, S. D.; Velev, O. D. An environmentally benign antimicrobial nanoparticle based on a silver-infused lignin core. Nat. Nanotechnol. 2015, 10, 817-823.

[0100] 25. Tassa, C.; Duffner, J. L.; Lewis, T. A.; Weissleder, R.; Schreiber, S. L.; Koehler, A. N.; Shaw, S. Y. Binding affinity and kinetic analysis of targeted small molecule-modified nanoparticles. Bioconjugate Chem. 2009, 21, 14-19.

[0101] 26. Joshi, P.; Shewale, V.; Pandey, R.; Shanker, V.; Hussain, S.; Karna, S. P. Tryptophan-Gold Nanoparticle Interaction: A First-Principles Quantum Mechanical Study. J. Phys. Chem. C 2011, 115, 22818-22826.

[0102] 27. Lacerda, S. H. D. P.; Park, J. J.; Meuse, C.; Pristinski, D.; Becker, M. L.; Karim, A.; Douglas, J. F. Interaction of Gold Nanoparticles with Common Human Blood Proteins. ACS Nano 2009, 4, 365-379.

[0103] 28. Copeland, R. A. Enzymes: A Practical Introduction to Structure, Mechanism, and Data Analysis; John Wiley & Sons: New York, N.Y., USA, 2004.

[0104] 29. Deng, H.; Gao, Y.; Dasari, T. P. S.; Ray, P. C.; Yu, H. A facile 3D construct of graphene oxide embedded with silver nanoparticles and its potential application as water filter. J. Miss. Acad. Sci. 2016, 61, 190-197.

[0105] 30. Tejamaya, M.; Römer, I.; Merrifield, R. C.; Lead, J. R. Stability of citrate, PVP, and PEG coated silver nanoparticles in ecotoxicology media. Environ. Sci. Technol. 2012, 46, 7011-7017.

[0106] 31. Sun, Y.; Xia, Y. Shape-Controlled Synthesis of Gold and Silver Nanoparticles. Science 2002, 298, 2176-2179.

[0107] 32. Liu, X.; Atwater, M.; Wang, J.; Huo, Q. Extinction coefficient of gold nanoparticles with different sizes and different capping ligands. Colloids Surf. B Biointerfaces 2007, 58, 3-7.

[0108] 33. Henglein, A.; Giersig, M. Formation of Colloidal Silver Nanoparticles: Capping Action of Citrate. J. Phys. Chem. B 1999, 103, 9533-9539.

[0109] 34. Santhi, A.; Umadevi, M.; Ramakrishnan, V.; Radhakrishnan, P.; Nampoori, V. Effect of silver nano particles on the fluorescence quantum yield of Rhodamine 6G determined using dual beam thermal lens method. Spectrochim. Acta A 2004, 60, 1077-1083.

[0110] 35. Chakraborty, M.; Panda, A. K. Spectral behaviour of eosin Y in different solvents and aqueous surfactant media. Spectrochim. Acta A 2011, 81, 458-465.

[0111] 36. Petrašek, Z.; Schwille, P. Precise measurement of diffusion coefficients using scanning fluorescence correlation spectroscopy. Biophys. J. 2008, 94, 1437-1448.

[0112] 37. Eftink, M. R.; Ghiron, C. A. Fluorescence quenching of indole and model micelle systems. J. Phys. Chem. 1976, 80, 486-493.

[0113] 38. Ghosh, D.; Chattopadhyay, N. Gold and silver nanoparticles based superquenching of fluorescence: A review. J. Lumin. 2015, 160, 223-232.

[0114] 39. Long, Z.; Liu, M.; Mao, L.; Zeng, G.; Huang, Q.; Huang, H.; Deng, F.; Wan, Y.; Zhang, X.; Wei, Y. One-step synthesis, self-assembly and bioimaging applications of adenosine triphosphate containing amphiphilies with aggregation-induced emission feature. Mater. Sci. Eng. C 2017, 73, 252-256.

[0115] 40. Quinn, S. D.; Dalgarno, P. A.; Cameron, R. T.; Hedley, G. J.; Hacker, C.; Lucocq, J. M.; Baillie, G. S.; Samuel, I. D. W.; Penedo, J. C. Real-time probing of β-amyloid self-assembly and inhibition using fluorescence self-quenching between neighbouring dyes. Mol. BioSyst. 2014, 10, 34-44.

[0116] 41. Lübtow, M.; Helmers, I.; Stepanenko, V.; Albuquerque, R. Q.; Marder, T. B.; Fernandez, G. Self-Assembly of 9,10-Bis(phenylethynyl) Anthracene (BPEA)

Derivatives: Influence of it-it and Hydrogen-Bonding Interactions on Aggregate Morphology and Self-Assembly Mechanism. Chem. A Eur. J. 2017, 23, 6198-6205.

[0117] 42. Nador, F.; Wnuk, K.; Roscini, C.; Solorzano, R.; Faraudo, J.; Ruiz-Molina, D.; Novio, F. Solvent-Tuned Supramolecular Assembly of Fluorescent Catechol/Pyrene Amphiphilic Molecules. Chem. A Eur. J. 2018, 24, 14724-14732.

[0118] 43. Huang, P.-C.; Mata, J. P.; Wu, C.-M.; Lo, C.-T. Morphology-Mediated Photoresponsive and Fluorescence Behaviors of Azobenzene-Containing Block Copolymers. Langmuir 2018, 34, 7416-7427.

[0119] 44. Lynch, I.; Salvati, A.; Dawson, K. A. Protein-nanoparticle interactions: What does the cell see? Nat. Nanotech. 2009, 4, 546-547.

[0120] 45. Al-Thabaiti, N. S.; Malik, M. A.; Khan, Z. Protein interactions with silver nanoparticles: Green synthesis, and biophysical approach. Int. J. Biol. Macromol. 2017, 95, 421-428.

1. A self-assembling nano-particle-based micelle composition, comprising a silver nanoparticle core and a plurality of layers of positively charged aromatic nitrogen-containing compounds.

2. A self-assembling nano-particle-based micelle composition according to claim **1**, wherein the silver nanoparticle is citrate-coated.

3. A self-assembling nano-particle-based micelle composition according to claim **1**, wherein the silver nanoparticle is present in solution at a concentration of about 1 μM or less, and the positively charged aromatic nitrogen-containing compounds are present in solution at a concentration of about 1 μM or less.

4. A self-assembling nano-particle-based micelle composition according to claim **1**, wherein the positively charged aromatic nitrogen-containing compounds are selected from the group consisting of dyes.

5. A self-assembling nano-particle-based micelle composition according to claim **1**, wherein the positively charged aromatic nitrogen-containing compounds are selected from the group consisting of Rhodamine 6G, Rhodamine B, and Methylene Blue.

6. A method for preparing self-assembling nano-particle-based micelle composition, comprising a silver nanoparticle core and a plurality of layers of positively charged aromatic nitrogen-containing compounds, said method comprising gradually adding a 1 μM solution of silver nanoparticle to a 1 μM solution of positively charged aromatic nitrogen-containing compound.

7. A method according to claim **6**, wherein the silver nanoparticle is citrate-coated.

8. A method according to claim **6**, wherein the positively charged aromatic nitrogen-containing compounds are selected from the group consisting of dyes.

9. A method according to claim **6**, wherein the positively charged aromatic nitrogen-containing compounds are selected from the group consisting of Rhodamine 6G, Rhodamine B, and Methylene Blue.

10. A method for aggregating positively charged aromatic nitrogen-containing compounds in solution, comprising adding silver nano-particles to a solution containing said positively charged aromatic nitrogen-containing compounds.

11. A method according to claim **10**, wherein said silver nano-particles are citrate-coated.

12. A method according to claim **10**, wherein said silver nano-particles are in solution at a concentration of about 1 μM or less.

13. A method according to claim **10**, wherein the positively charged aromatic nitrogen-containing compounds are selected from the group consisting of dyes.

14. A method according to claim **10**, wherein the positively charged aromatic nitrogen-containing compounds are selected from the group consisting of Rhodamine 6G, Rhodamine B and Methylene Blue.

* * * * *